High-frequency electron spin resonance in Kagome-Lattice YMn_6Sn_6

IOP Publishing J. Phys.: Condens. Matter 38 (2026) 095801 https://doi.org/10.1088/1361-648X/ae4867

Journal of Physics: Condensed Matter

PAPER

High-frequency electron spin resonance in Kagome-Lattice YMn_6Sn_6

Lovia Ofori[1], Johan Van Tol[2], Nathan Tolva[3], Hari Bhandari[4,5], Nirmal J Ghimire[4,5] and Srinivasa Rao Singamaneni[1,*]

[1] Department of Physics, The University of Texas at El Paso, El Paso, TX 79968, United States of America
[2] National High Magnetic Field Laboratory, Florida State University, Tallahassee, FL 32310, United States of America
[3] Department of Physics, Boston College, Chestnut Hill, MA 02467, United States of America
[4] Department of Physics & Astronomy, University of Notre Dame, Notre Dame, IN 46556, United States of America
[5] Stavropoulos Center for Complex Quantum Matter, University of Notre Dame, Notre Dame, IN 46556, United States of America
[*] Author to whom any correspondence should be addressed.

E-mail: srao@utep.edu

Keywords: Kagome magnets, electron spin resonance, magnetism, spin correlations

OPEN ACCESS

RECEIVED
29 August 2025

REVISED
28 January 2026

ACCEPTED FOR PUBLICATION
19 February 2026

PUBLISHED
3 March 2026

Abstract

Metallic Kagome magnets have received a great deal of research attention in recent years for their intriguing magnetic properties. Recently, YMn_6Sn_6 (Y166), which belongs to this family of compounds, has been studied to show different magnetic phases including the distorted spiral (DS), transverse conical spiral (TCS), fan-like (FL) and the forced-ferromagnetic (FF) phases respectively. In this work, we employed very high-frequency electron spin resonance (VHF-ESR) spectroscopy to investigate the local microscopic magnetic interactions of Mn ions in Y166. Particularly, the temperature-dependent ESR behavior at variable very-high microwave frequency ($\nu = 120$, 240, and 300 GHz) was studied. The ESR spectral behavior above room temperature (up to 350 K) on Y166 single crystals, where the magnetic field was applied in-plane and out-of-plane orientations of the sample layers was also investigated. A couple of non-trivial magnetic phases at different temperatures and frequencies, including the TCS, FL and FF phases were identified. The DS phase was not identified because our measurements were taken at fields higher than the fields (0-2 T) at which this phase occurs. In addition, angular dependence of the resonance field at room temperature (290 K) for $\nu = 240$ GHz follows a $(3\cos^2\theta - 1)$- like angular dependence which reveals the 'U-shape' (from 0° to 180°) of the resonance field. This behavior indicates the presence of 2D spin correlations in Y166. This work has implications in emerging applications such as high-frequency microwave and terahertz communications and spintronics.

1. Introduction and motivation

Recent research has focused on Kagome lattice magnets, particularly RT_6Sn_6 compounds, where R is a rare-earth element and T is a 3d transition metal element, due to their unique magnetic and electrical characteristics. Y166 is among these compounds, characterized by competing magnetic phases, topological Hall effect, Dirac bands, emergent electromagnetic induction, and anomalous transverse thermoelectric effect [1, 2]. This has led to increased interest in these materials. Y166 undergoes a transition to a commensurate antiferromagnetic state below 345 K, and subsequently orders into an incommensurate spiral state below 333 K [1, 3]. Y166 is an excellent metal and has a hexagonal structure made up of Kagome planes divided by Sn_3 and YSn_2 layers, belonging to a class of materials that can support a wide range of topological states and phenomena. In the crystal structure, the Mn atoms form a Kagome net in the basal plane of the hexagonal space group P6/mmm (191) [1]. Ghimire *et al* reported the emergence of non-trivial magnetic phases in Y166 that were obtained from susceptibility measurements at different temperatures. They denoted the distorted spiral (DS), transverse conical spiral (TCS),

fan-like (FL), and forced FM (FF), respectively, based on the magnetic structures observed [1]. Y166 exhibits a large anomalous transverse thermoelectric effect that is higher than that of other antiferromagnetic systems that are comparable to ferromagnetic systems [4]. High-frequency electron spin resonance (HF-ESR) has been reported on several different compounds to investigate their electronic and magnetic properties. This spectroscopic technique is a useful tool for investigating the rich magnetic behavior of van der Waals compounds because of its exceptional energy resolution and high sensitivity to magnetic anisotropies, which together allow for in-depth understanding of the low energy spin dynamics in the ordered and paramagnetic phases as well as the specifics of the spin structure in the magnetically ordered state [5]. Mehlawat *et al* reports the use of high-frequency/high-magnetic field ESR experiments on single crystals of the quasi-two-dimensional antiferromagnet $Ni_2P_2S_6$ to reveal anisotropic spin fluctuations and a low-energy magnon excitation [6]. Another study used HF-ESR spectroscopy analyzed magnetic interactions in a plate-like CrX_3 system (X = Cl, Br, I). They found that the Ginzburg–Landau critical model adequately describes the temperature dependence of the ESR linewidth, which indicates the presence of 2D spin correlations [7]. A recent work has been reported in which the authors employ the use ferromagnetic resonance spectroscopy applied to Kagome magnet $MgMn_6Sn_6$ [8] to study and quantify the intrinsic magneto crystalline anisotropy that is responsible for the alignment of the Mn magnetic moments in the Kagome plane. Their findings show that the external shape anisotropy, due to the plate-like structure of the crystal, has a small effect. In contrast, the intrinsic uniaxial magneto crystalline anisotropy, which arises from spin–orbit coupling and is of the easy-plane kind, is much more significant [8].

While results of high frequency ESR have been reported for these similar materials, no HF-ESR study has been reported on the Kagome magnet Y166. In this work, we make use of HF-ESR to investigate the local microscopic magnetic properties of Mn ions in Y166 to better understand new observed magnetic phases or textures. While it is challenging to measure ESR in these metallic systems, the high frequencies and fields allow to probe different parts of the magnetic phase diagram. Particularly we studied ESR properties at a few microwave frequencies, ν = 120, 240 and 300 GHz, respectively. We also have investigated the ESR spectral behavior above room temperature on Y166 single crystals, where the magnetic field was applied within both the in-plane (IP) and out-of-plane orientations (OOP) of the sample layers [9]. In addition, we have performed ESR at ν = 240 GHz to study the angular dependence of the resonance field and linewidth. The temperature dependencies of signal behavior, signal breadth, and g-values were tracked to study the magnetic phase transition in the Y166 compound as a function of temperature from 5 to 350 K at ν = 120, 240 and 300 GHz. Our findings may indicate the presence of 2D spin fluctuations in Y166 [1, 7].

2. Experimental details

Y166 single crystals were grown using the self-flux technique [1]. HF-ESR measurements were conducted at the National High Magnetic Field Laboratory (NHFML) to sufficiently capture the full ESR spectrum as the magnetic anisotropy of this compound is higher than the typical X-band frequency (9.84 GHz). The HF-ESR spectrometer at the NHFML allows for comprehensive analysis, providing deeper insights into the magnetic characteristics of the sample, as HF-ESR can capture the full ESR spectra of this compound. This system utilizes a superheterodyne spectrometer with a multi-frequency quasioptical submillimeter bridge and a sweepable 12.5 T superconducting magnet [7]. The spectrometer operates in reflection mode, and no resonator was used, which is essential for this metallic sample. HF-ESR measurements were conducted on a Y166 single crystal of approximate dimension 4 × 4 × 0.5 mm as a function of temperature at υ = 120, 240 and 300 GHz from T = 5 K to 350 K where the sample was placed both in the IP and OOP orientation with respect to the magnetic field. For these measurements, the sample was placed in a rexolite sample holder with vertical and horizontal slots for the sample respectively. Measurements as a function of angle θ (degrees) were also conducted at T = 290 K for υ = 240 GHz. The sample was placed inside the instrument attached to a PEEK sample rotator and rotated along the axis perpendicular to the sample (c-axis) for the measurements. Figure 1(a) shows the Y166 crystal structure. Figure 1(b) shows an overhead view of the structure depicted in figure 1(a) showing the Kagome net of Mn atoms. Two Kagome planes with the formula Mn_3Sn, divided by Sn_3 and YSn_2 layers, are present within a unit cell represented by the gray solid lines [1]. Y166 crystal placed on a sample holder is shown in figure 1(c) with the rotation angle along the length of the holder [9].

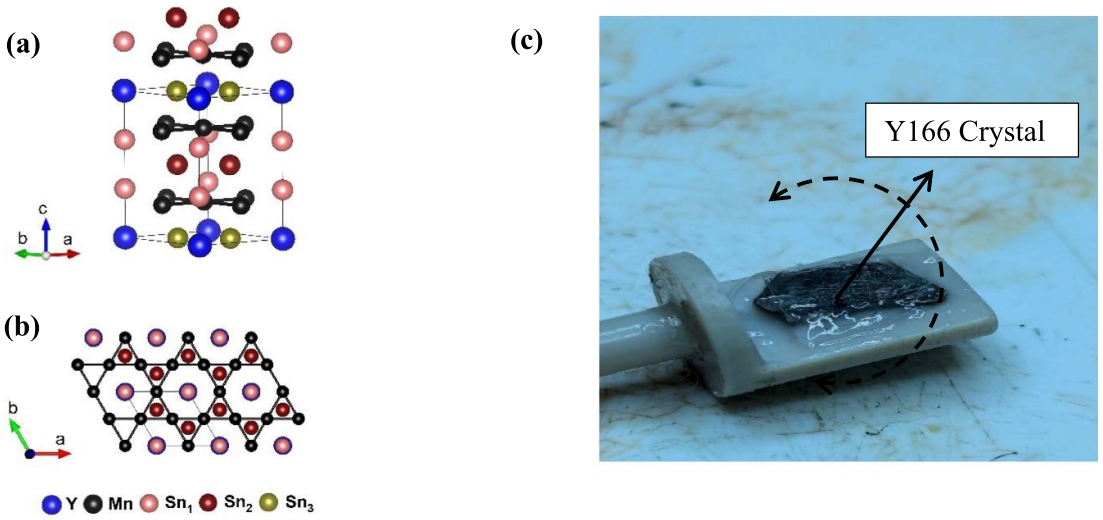

Figure 1. Hexagonal crystal structure (a) and top view (b) of Y166 showing the Kagome net of Mn atoms. The crystal structure data were obtained from [1]. (c) Y166 placed on a sample holder. Reproduced with permission from [9].

3. Results and discussion

3.1 Temperature dependent ESR study of Y166 at different frequencies ($\nu = 120$, 240 and 300 GHz)

The recent magnetization study reported by Ghimire *et al* [1] reveals different magnetic phases in Y166 at varying temperatures and magnetic fields, with metamagnetic transition fields shifting to lower fields as a function of temperature [1]. We notice this same behavior in our HF-ESR studies as shown in figure 2. By investigating the ESR at different microwave frequencies we study different field ranges in the phase diagram, 3.5–5.5 T at 120 GHz, 6.5–10.5 T at 240 GHz, and 9.5–12.5 T at 300 GHz. Figure 2(a) shows the temperature dependent ESR spectra of Y166 at 120 GHz, for the IP orientation of the magnetic field. At low temperatures, the resonance is close to $g \approx 2$ and shifts towards lower resonance fields with increasing temperature up to ∼275 K. Above this temperature, the shift reverses and moves to higher field, signaling the transition from the TCS phase into the FF phase. The resonance field in the OOP orientation is centered at a higher field of ∼5.4 T, with a significant shift towards higher fields as temperature increases as shown in figure 2(b) [9]. At low temperatures, below ∼180 K, no resonance from Y166 is observed, except for a small signal due to paramagnetic impurity at $g = g_e$, which appears to come from the background of the sample holder, which is not discussed further. Above 180 K, there is a strong temperature dependence of the resonance field with a shift towards higher fields as temperature increases up to ∼260 K.

The OOP ESR spectra are broader than that of IP spectra, which is consistent with nonuniform demagnetization in our non-ideal, finite-thickness sample. Below ∼180 K, the OOP signal disappears due to reduced transverse susceptibility in the TCS phase. The TCS phase [1, 9] occurs below 250 K and 3.6 T with a reduction in the net magnetization due to the cycloidal arrangement of spins, where the spins are tilted along the direction of the applied external magnetic field, forming a transverse conical structure [1, 9]. The FF [1] phase occurs above 250 K, causing a shift in resonance field in both orientations. Above the transition temperature, the transition shifts to lower fields, indicating a decrease in magnetization and the magnetization in the FF phase is not fully saturated at higher temperatures [9]. Around 240–260 K; two distinct peaks are discernable in the spectra corresponding to the TCS and the FF phases in the OOP orientation. The phase II as reported in [1] appears to be a region where these two magnetic phases coexist. It should be noted that for the reported resistivity values, [1] the skin depth of the milli waves range from about 2 μm at high temperatures to a few hundred nanometers at low temperatures, this skin depth will decrease further at higher frequencies with the square root of the wavelength [1].

Figures 2(c) and (d) show the temperature dependent ESR spectra of Y166 at 240 GHz for IP and OOP orientations. At 240 GHz, the resonances occur at higher fields, and for both orientations the deviations from $g \sim 2$ gradually increase upon lowering the temperature down to around 125 K (at ∼7.5 T) for IP direction and to ∼100 K (at ∼10.5 T) for the OOP direction. The FF phase exists down to lower temperatures (in both orientations) and starts approaching the ferromagnetic saturation field. For the IP orientation (as shown in figure 2(c)), the transition from the FF to the FL phase is observed around

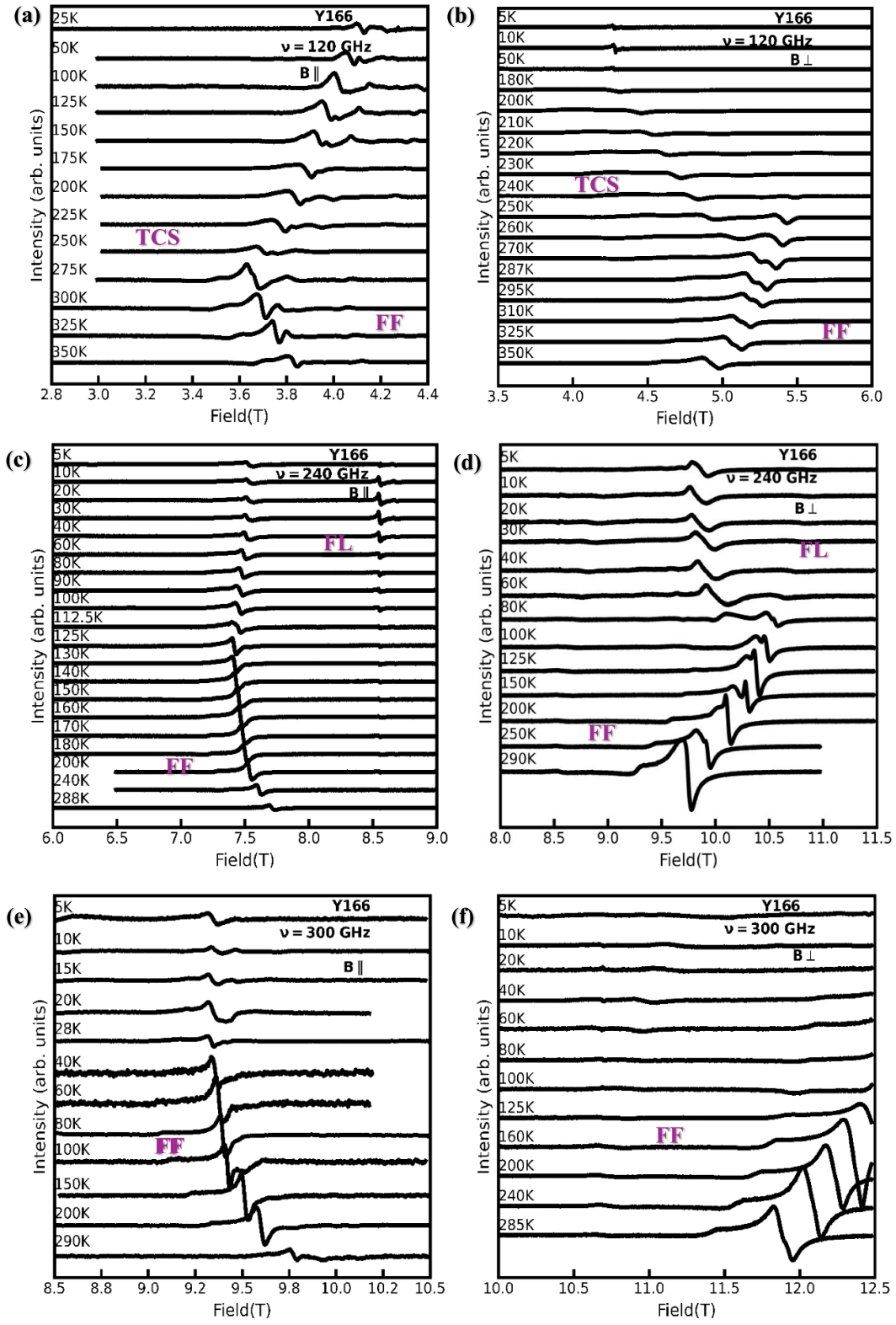

Figure 2. Temperature-dependent ESR spectra of Y166 measured at three microwave frequencies: (a), (b) 120 GHz for in-plane and out-of-plane orientations; (c), (d) 240 GHz for in-plane and out-of-plane orientations; (e), (f) 300 GHz for in-plane and out-of-plane orientations. The phases shown (in magenta) suggest the presence of phase transitions in Y166, whose positions vary with frequency, sample orientation and temperature.

125 K. With decreasing temperature below 125 K, the resonance field slightly shifts to higher fields to 7.5 T. This slight shift indicates that in the FL phase the magnetization in the field direction is relatively stable as a function of temperature, while the linewidth slightly narrows at lower temperatures. The signal at 8.56 T is paramagnetic background signal from the sample holder. For the OOP direction shown in figure 2(d), the transition from the FF phase to the FL occurs at a slightly lower temperature than

for the IP direction as we are at higher magnetic field. Again, a transition region seems to be present between 100 and 60 K where signals from both FL and FF phases are observed, possibly corresponding to the intermediate phase I [1]. The signal in the FL phase shifts to slightly lower field values below 80 K and is relatively stable at 9.9 T below 40 K.

Figures 2(e) and (f) show the temperature dependent ESR spectra at 300 GHz for IP and OOP. At 300 GHz, Y166 approaches saturation of the local magnetization at the Mn sites because of the higher applied magnetic fields, causing it to remain in the FF phase at lower temperatures. Figure 2(e) (IP orientation) shows a gradual shift towards lower resonance fields, approaching ∼9.35 T as the temperature decreases, with no observation of a phase transition.

For the OOP orientation measured at 300 GHz shown in figure 2(f), no signal could be observed below ∼125 K, as the resonance field shifts outside the available field range of 12.5 T. Y166 exhibits ferromagnetic behavior at higher resonance fields throughout the temperature range, as seen in figure 2(f). The large difference between the IP and OOP resonances ($\Delta B \approx 1.8$ T) shows the local demagnetization field at the Mn sites. The dipolar field experienced by a Mn spin is highly anisotropic because the Mn ions lie in layers on the Kagome plane, which resulted in two distinct observations. Firstly, for OOP orientation, all Mn neighbors produce a *negative* dipolar field, shifting the resonance to higher external field which corresponds to an effective demagnetization factor of +1. Secondly, for IP orientation, some neighbors contribute positively and others negatively, giving a net *positive* internal field that shifts the resonance to lower external field, corresponding to an effective demagnetization factor of −0.5 [10]. Using the thin-crystal relation $\Delta B = N_\Delta\, M_{\rm loc}$ with $N_\Delta = (1—(–0.5)) = 1.5$, the local magnetization at ∼275 K is:

$$M_{\rm loc} = \frac{\Delta B}{N_\Delta} = \frac{1.8}{1.5} \approx 1.2\ \text{T}. \tag{1}$$

The *average* resonance field is:

$$B_{\rm avg} = \frac{2B_{\rm IP} + B_{\rm OOP}}{3} = 4.2\ \text{T}. \tag{2}$$

This gives a corresponding *g*-value:

$$g = \frac{h\nu}{\mu_{\rm B} B_{\rm avg}} \approx 2.04. \tag{3}$$

At 125 K, the IP and OOP resonances occur at approximately 7.45 T and 10.35 T, giving:

$$\Delta B = 2.90\ \text{T},\ M_{\rm loc} = \frac{2.90}{1.5} \approx 1.93\ \text{T}.$$

The average resonance field is, yielding:

$g \approx 2.04$. Thus, the same *g*-value describes all FF-phases across frequencies. The larger shifts at 240 GHz compared to 120 GHz reflect a larger local magnetization in the FL and FF phases at higher fields. As the temperature rises from 125 K to 290 K, the signal broadens [9]. This broadening is more pronounced around 200 K, which might indicate an increase in spin fluctuations at higher temperatures.

In the FF phase, we can treat the resonance positions as a ferromagnetic resonance with the shifts of the resonance fields from the expected single ion field position ($B_0 = h\nu/g\mu_{\rm B}$) determined by the magnetization and the sample shape. For Y166, we could not measure the *g*-value in the paramagnetic phase (above 345–350 K) as the spectra was measured within our available temperature range (5–350 K), and therefore the *g*-value was estimated from the ferromagnetic signals. We approximate our thin single crystal as a thin film with demagnetization factors of 1 for the OOP direction and 0 for the IP directions. We assumed that the *g*-value is isotropic and estimated it from the average resonance fields in the FF phase, $B_0 = (2^*B_{\rm IP} + B_{\rm OOP})/3$, giving an average *g*-value of 2.04, which is within the typical range for 3d transition metal ions. The deviation from the free electron value is due to single ion spin–orbit coupling in the local crystal field environment and can be expected to be largely field and temperature independent. In the limit of $B \gg \mu_0$M, the ferromagnetic resonance for an isotropic thin plate is shifted to higher magnetic field by μ_0M for the OOP direction and shifted to lower magnetic field by 0.5 μ_0M [10].

Using the same intrinsic $g = 2.04$ (for which the average resonance field is $B_{\rm avg} = 10.5$ T), the local magnetization at the Mn positions can be estimated from the low temperature signal in the IP direction at 300 GHz: $\mu_0 M_{\rm loc}$ is 2.3 T. This corresponds roughly to the value of the extrapolated resonance field

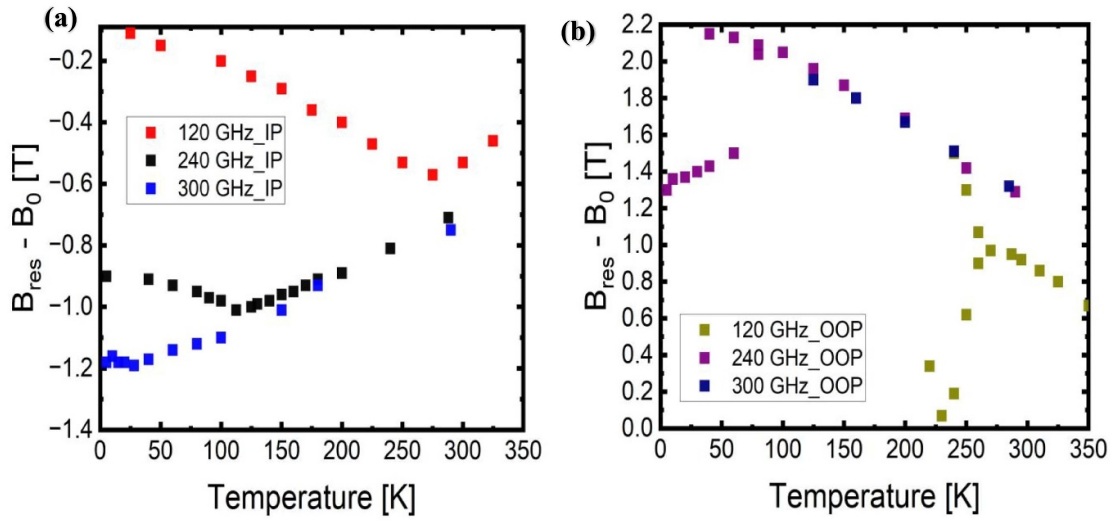

Figure 3. Temperature dependence of the resonance field deviation $\boldsymbol{B_{res}}$—$\boldsymbol{B_0}[\boldsymbol{T}]$ for Y166. (a) In-plane (IP) orientation at microwave frequencies of 120 GHz (**red**), 240 GHz (**black**), and 300 GHz (**blue**). (b) Out-of-plane (OOP) orientation at microwave frequencies of 120 GHz (**dark yellow**), 240 GHz (**purple**), and 300 GHz (**navy**). The quantity $\boldsymbol{B_0}$ corresponds to the average field ($\boldsymbol{B_{avg}}$) at which $g = 2.04$.

for the OOP directions for both 240 GHz and 300 GHz, which is about 2.3 T times higher than the resonance field for a g-value of 2.04

$$M_{\text{loc}} = \frac{B_0 - B_{\text{IP}}}{|\, N_{\text{IP}} \,|} = \frac{10.5 - 9.35}{0.5} \approx 2.3\ \text{T},$$

which is the largest local magnetization observed, consistent with the fact that at higher applied fields, there is full alignment of the Mn moments in the FF phase.

Figures 3(a) and (b) show the deviations of B_{res} (the measured resonance field) from B_0 (the resonance field for $g = 2.04$) for the IP and OOP orientations of Y166 crystal as a function of temperature for all three frequencies (120, 240, 300 GHz). At all frequencies and temperatures, the resonance for the IP orientation is shifted to lower fields with respect to the expected single ion resonance, while for the OOP direction the resonances occur at higher fields. This is typical for a ferromagnetic resonance of a thin sample and can be understood as the contribution of the dipolar field of the surroundings of the spins. The negative deviation in the IP orientation suggests that internal dipolar fields are assisting the external field, so resonance is reached at lower fields. This means that to achieve resonance, a greater external field is required. Our sample is not an ideal infinitely thin sample which might contribute to the linewidth of the resonances. Also, resonances are not ideal Lorentzian or Dysonian but have a more complex line shape and weak additional features can be due to the finite thickness and features from the edge of the sample as shown in figure 2. Also, the limited penetration depth (skin depth) of the millimeter waves can play a role. At 120 GHz in the 240–260 K temperature range and at 240 GHz around 40–80 K temperature range, two resonance modes appear to coexist. These regions correspond to the transitions between the FF and TCS phases and the FF and FL phases, respectively, and might correspond to the intermediate phases II and I that were identified by Ghimire *et al* [1]

3.2 Angular dependent ESR study of Y166 at 240 GHz and 290 K

We now show the angular dependence of Y166 at a frequency of 240 GHz and a fixed temperature of 290 K. Here, we observe the variations in the ESR signals and the resonance field as function of angle. In figures 4(a) and (b) presented below, the resonance field shifts significantly as the angle varies, ranging from approximately 7.7 T to 9.7 T. The signals vary significantly as a function of angle of rotation, becoming broader at certain angles. The sharp signals that arise at 162°, 171° and 180° at 8.4 T (where $g = 2$) are likely due to impurities arising from sample holder and will not be discussed further. The intensity at angles away from zero degrees (OOP) drops significantly due to instrumental effects. As the measurement is performed in reflection mode and the sample is reflective and larger than the wavelength, much less of the reflected signal will be traveling back in the waveguide at angles deviating significantly from the OOP direction. The $g = g_e$ background signal is more pronounced at 180°, as the microwaves go through the sample holder before being reflected from the sample, while at 0°,

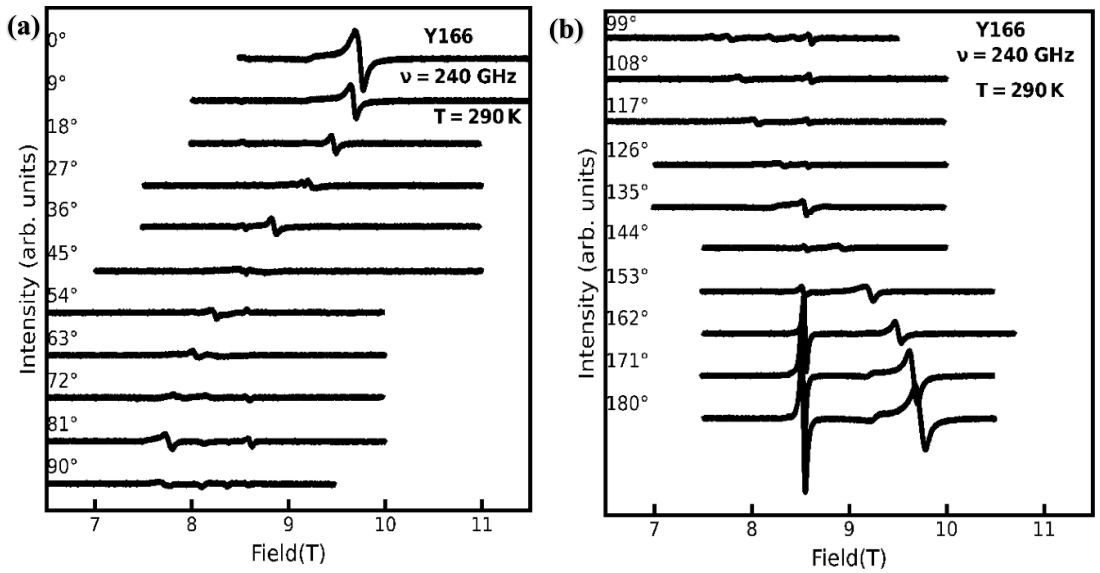

Figure 4. Angular dependence of ESR spectra of Y166 measured at $T = 290$ K and $\nu = 240$ GHz in the OOP orientation. (a) Spectra for rotation angles from 0° to 90°; (b) Spectra for rotation angles from 99° to 180°. Each spectrum corresponds to a different sample orientation relative to the external magnetic field. The systematic evolution of the resonance position and line shape with respect to angle reflects the anisotropic magnetic environment of Y166.

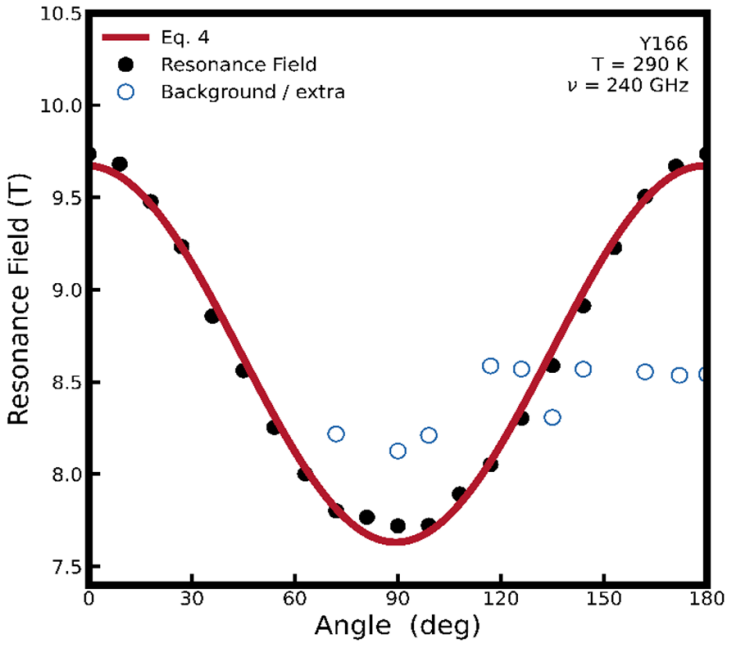

Figure 5. Angular dependence of the resonance field of Y166 measured at $T = 290$ K and $\nu = 240$ GHz. The red dots represent the experimentally obtained resonance fields as a function of rotation angle. The black curve shows a fit to the modified form of equation (1), $H_{\rm res}\ (\theta) = [F(3\cos^2\theta - 1) + G]$, which accounts for a phase shift ϕ. The blue opened circles represent the background or weak signals that were obtained from fitting the multiple peaks shown in figure 4, using multiple Lorentzian fits.

the microwaves are reflected from the front surface of the sample, and the microwaves 'see' less of the sample holder that it is mounted on as shown in figure 1(c). At some orientations around 90°, the signal is less well defined, and some additional features appear. At these angles irregularities on the thin side surface of the sample might give enhanced contributions.

The resonance field (red circles, left y-axis) as a function of angle measured at a fixed temperature of 290 K is shown in figure 5. The angular dependence of the resonance field is fitted with the simple model [7],

$$H_{\rm res}\ (\theta) = F\left(3\cos^2\theta - 1\right) + G. \tag{4}$$

The $(3\cos^2\theta - 1)$-like behavior is characteristic of 2D systems [11, 12]. This 'U-shape' behavior (from 0° to 180°) of the resonance field has also been previously observed in materials such as CrSBr, K_2MnF_4, $CrCl_3$ and CrI_3 which exhibit 2D Heisenberg behavior and correlations suggesting a weak XY model [7, 11–13]. The curve that joins the values of the resonance fields is obtained from the fit using (4). The resonance field varies significantly as a function of the angle of rotation, indicating strong angular dependence. This resonance field shape suggests anisotropic magnetic behavior, likely due to the crystal field or spin–orbit coupling effects. The angular dependency of the resonance field at this temperature can be attributed to the sample shape in combination with the non-cubic distribution of dipoles in the 2D lattice. The net dipolar field shifts the resonance field according to (equation (4) [12]. The scattered points in the resonance field (indicated with open blue circles) were obtained from fitting the multiple peaks shown in figure 4, using multiple Lorentzian fits.

A straight comparison of our HF-ESR results with the neutron diffraction and magneto transport study by Ghimire *et al* [1] provides a consistent picture of the magnetic phases in the Kagome metal Y166. While Ghimire *et al* constructed the magnetic phase diagram using bulk magnetization, Hall resistivity, and neutron scattering, our HF-ESR measurements probe the local magnetic environment and dynamic response of Mn spins at different microwave frequencies and orientations. Ghimire *et al* identified four principal field-induced phases, thus the DS, TCS, FL and forced-ferromagnetic (FF) phases, where the fields were applied in the *ab* plane with metamagnetic transition fields $H_1 \approx 2$ T, $H_2 \approx 6$–7 T, and $H_3 \approx 9$–10 T [1]. Our HF-ESR measurements, taken at fixed frequencies corresponding to resonance fields of 3.5–6.5 T (120 GHz), 6.5–10.5 T (240 GHz), and 9.5–12.5 T (300 GHz), naturally observe the TCS, FL, and FF regions which lie above the DS phase, explaining its absence in our spectra. The observed resonance shifts, linewidth changes, and intensity variations correlate well with the transition fields reported in their study. Moreover, for $H \parallel c$, our OOP ESR spectra display smoother shifts and broader lines, aligning with their observation of a continuous evolution from a helical to longitudinal conical spiral state without abrupt metamagnetic steps [1]. Overall, the local dynamic information obtained from our HF-ESR complements the static spin-structure mapping from their neutron diffraction measurements. Both approaches consistently identify the TCS, FL, and FF phases and confirm that thermal spin fluctuations within the quasi-two-dimensional Mn layers play a key role in the field-induced magnetic behavior of Y166. The large local magnetization in the FF phase that we obtain from our data would correspond to μB/Mn, which is substantially larger than what is obtained from the magnetization and susceptibility measurements. That is due to the layered structure with the Mn–Mn distances in the layers substantially shorter than those in the *c*-direction. This enhances the local dipolar fields. In the FF and TCS phases, the simple ferromagnetic approach cannot be applied, but our data indicates that in the FL phase, the spin has a significant component in the field direction, of which the local dipolar fields at the Mn sites is about 60%–75% of the saturation field. On the contrary, in the TCS phase (below 230K at 120 GHz), the local dipolar fields seem to converge to zero at low temperature.

4. Conclusion

HF-ESR spectroscopy was conducted on the Kagome magnet Y166 to study local magnetic interactions of Mn ions and new observed magnetic phases at different microwave frequencies. We observed that Mn ions are responsible for ESR signal and magnetic properties in Y166, with different phase transitions occurring at different temperatures for each microwave frequency and magnetic field range aligning with Ghimire *et al* work [1]. The TCS phase is observed at lower temperatures below 250 K and 3.6 T field, while the FL phase is observed at 80 K and higher field of 10.35 T. The Forced Ferromagnetic phase is observed at higher temperatures of 250 K and above, and at a higher field of 12.5 T. Our ESR results indicate that the transition phases I and II in [1] could be due to a coexistence zone of the phases FF and FL; and FF and TCS phases respectively, with a gradual transition of the fractions of these phases. Our angular dependence results reveal that the resonance field follows a $(3\cos^2\theta - 1)$-like dependence at room temperature. Our results have highlighted the importance of using HF-ESR to expand our understanding of magnetic correlations and anisotropies in Kagome systems. To the best of our knowledge, ESR has never been used to investigate the local microscopic magnetic interactions of Mn ions in Y166, and we hope our results will pave way for the combination of ESR and other microscopy or magnetization techniques to further investigate the magnetic properties and domains in these Kagome systems.

Acknowledgments

S.R.S. and L.O. acknowledge support from the NSF-DMR (Award No. 2105109). The National High Magnetic Field Laboratory is supported by National Science Foundation through NSF/DMR-2128556 and the State of Florida. S.R.S. and L.O. acknowledge support from NSF-MRI (Award No. 2018067). N.J.G acknowledges the support from the NSF CAREER award DMR-2343536. The author's master's thesis, *'Investigation of High-Frequency Electron Spin Dynamics in the Kagome-Lattice YMn_6Sn_6 Crystal,'* which was submitted to The University of Texas at El Paso in 2025 and is accessible via ProQuest, contains portions of this work. Beyond what is stated in the thesis, the current manuscript offers more in-depth study and improved interpretations.

Data availability

The data that support the findings of this study are openly available at the following URL/DOI:. URL/DOI: https://osf.io/3f82s/files/osfstorage/?view_only=b7098096e53547c8be87b6aba5c91212 [14].

ORCID iDs

Lovia Ofori 0009-0005-8877-9040
Johan Van Tol 0000-0001-6972-2149
Srinivasa Rao Singamaneni 0000-0003-1653-9759

References

[1] Ghimire N J *et al* 2020 Competing magnetic phases and fluctuation-driven scalar spin chirality in the Kagome metal YMn_6Sn_6 *Sci. Adv.* **6** eabe2680
[2] Bhandari H, Dally R L, Siegfried P E, Regmi R B, Rule K C, Chi S, Lynn J W, Mazin I I and Ghimire N J 2024 Magnetism and fermiology of Kagome magnet $YMn_6Sn_4Ge_2$ *npj Quantum Mater.* **9** 6
[3] Kitaori A, Kanazawa N, Yokouchi T, Kagawa F, Nagaosa N and Tokura Y 2021 Emergent electromagnetic induction beyond room temperature *Proc. Natl Acad. Sci.* **118** e2105422118
[4] Roychowdhury S, Ochs A M, Guin S N, Samanta K, Noky J, Shekhar C, Vergniory M G, Goldberger J E and Felser C 2022 Large room temperature anomalous transverse thermoelectric effect in Kagome antiferromagnet YMn_6Sn_6 *Adv. Mater.* **34** 2201350
[5] Kataev V, Büchner B and Alfonsov A 2024 *Electron Spin Resonance Spectroscopy on Magnetic van der Waals Compounds* (Springer) (https://doi.org/10.1007/s00723-024-01671-x)
[6] Mehlawat K, Alfonsov A, Selter S, Shemerliuk Y, Aswartham S, Büchner B and Kataev V 2022 Low-energy excitations and magnetic anisotropy of the layered van der Waals antiferromagnet *Phys. Rev. B* **105** 214427
[7] Saiz C L, Delgado J A, Van Tol J, Tartaglia T, Tafti F and Singamaneni S R 2021 2D correlations in the van der Waals ferromagnet $CrBr_3$ using high frequency electron spin resonance spectroscopy *J. Appl. Phys.* **129** 233902
[8] Pal R, Deb K, Kumar N, Büchner B, Alfonsov A and Kataev V 2025 Ferromagnetic resonance spectroscopy on the Kagome magnet $MgMn_6Sn_6$ *Appl. Magn. Reson.* **56** 1507–21
[9] Ofori L and Rao Singamaneni S 2025 Investigation of high-frequency electron spin dynamics in the Kagome-Lattice YMn_6Sn_6 crystal *Master's Thesis* University of Texas at El Paso (available at: https://utep.idm.oclc.org/login?url=www.proquest.com/dissertations-theses/investigation-high-frequency-electron-spin/docview/3215574286/se-2?accountid=7121)
[10] Kittel C 1948 On the theory of ferromagnetic resonance absorption *Phys. Rev.* **73** 155–61
[11] Richards P M and Salamon M B 1974 Exchange narrowing of electron spin resonance in a two-dimensional system *Phys. Rev. B* **9** 32–45
[12] Chehab S, Amiell J, Biensan P and Flandrois S 1991 Two-dimensional ESR behaviour of CrCl3 *Physica B* **173** 211–6
[13] Moro F, Ke S, Del Águila A G, Söll A, Sofer Z, Wu Q, Yue M, Li L, Liu X and Fanciulli M 2022 Revealing 2D magnetism in a bulk CrSBr single crystal by electron spin resonance *Adv. Funct. Mater.* **32** 2207044
[14] Ofori L and Singamaneni R 2026 HF-EPR Data *Open Science Framework (OSF)* (https://doi.org/10.17605/OSF.IO/3F82S)